



Synthesis, Biological Activity, and Computational Examination of New 3-Cyano-2-oxa-pyridine Derivatives

Kawkab A Hussein*, Zainab Al-Shuhaib, Sadiq M. H. Ismael

Department of Chemistry, College of Education for Pure Sciences, University of Basrah, Basrah, Iraq

ARTICLE INFO*Article history:*

Received 5 September 2023

Revised 20 October 2023

Accepted 08 November 2023

Published online 01 December 2023

Copyright: © 2023 Hussein *et al.* This is an open-access article distributed under the terms of the [Creative Commons Attribution License](https://creativecommons.org/licenses/by/4.0/), which permits unrestricted use, distribution, and reproduction in any medium, provided the original author and source are credited.

ABSTRACT

Numerous studies have been carried out into the chemistry of condensed heterocyclic compounds in terms of their medication discovery and various biological properties. Pyridines play an essential role in medicinal chemistry because they are widely available as natural compounds and have served as the foundation for several drugs on the market. In the current investigation, 3-cyano-2-oxa-pyridine derivatives 4a-e were synthesized by a one-pot multicomponent reaction, starting from substituted acetophenone, ethyl cyanoacetate, and aryl aldehydes in the presence of ammonium acetate. All the new products were subjected to proton nuclear magnetic resonance (¹H NMR), carbon nuclear magnetic resonance (¹³C NMR), two-dimensional (2D)-NMR analysis using heteronuclear single quantum coherence spectroscopy (HSQC), and electron ionization (EI-MS). Additionally, an *in vitro* cytotoxicity test was performed on cervical carcinoma (HeLa) and cerebral glioblastoma multiforme (AMGM5) cells for every produced molecule. The results indicated that the tested compounds 4a, 4c, and 4e inhibited AMGM5 cells with average IC₅₀ values of 656.4, 781.5, and 374.5 μM, respectively. Compounds 4a, 4b, and 4e, on the other hand, showed a cytotoxic action against the HeLa cell line, with average IC₅₀ values of 558.5, 775.6, and 615.9 μM, respectively. The optimized geometry and reactivity descriptors were also analyzed, including the highest occupied molecular orbital (HOMO), least unoccupied molecular orbital (LUMO), energy band gap (ΔE), chemical potential (μ), electronegativity (χ), chemical hardness (η), chemical softness (S), and electrophilicity (ω). The experimental outcomes of the biological evaluation were consistent with the results of the investigation into their molecular modeling.

Keywords: Anticancer, Cyano-pyridines, Multicomponent reaction, DFT, Pharmacokinetics.

Introduction

Pyridine products have long been studied due to the abundance of pyridine in nature and its widespread use as the structural core of numerous medicinal pharmaceuticals.^{1,2} These natural and manmade compounds have numerous uses in medication research and functional materials.^{3,4} This has contributed to the creation of physiologically relevant heterocyclic compounds such as pyridine analogues.⁵ Additionally, pyridine analogues are essential heterocyclic molecules with pharmacological and functional features that make them appealing as medicines and general synthetic building blocks.^{6,7} The pyridine core is found in anti-inflammatory and anticancer drugs.⁸ Anticancer medicines have been described as being comprised of pyridine derivatives, including different groups such as streptonigrone, streptonigrin, and lavendamycin, while cerivastatin has been reported as a hydroxymethylglutaryl-CoA reductase enzyme inhibitor.⁹ Furthermore, substituted pyridines have been found to be leukotriene B-4 antagonists.¹⁰ Cyanopyridine derivatives, on the other hand, have been demonstrated to have antibacterial,¹¹ antioxidant,¹² antibiotic,¹³ anti-inflammatory,¹⁴ analgesic,¹⁵ anticonvulsant,¹⁶ and anticancer¹⁷ effects.

*Corresponding author. E mail: kawkab.ali@uobasrah.edu.iq
Tel: +9647700669032

Citation: Hussein KA, Al-Shuhaib Z, Ismael SMH. Synthesis, Biological Activity, and Computational Examination of New 3-Cyano-2-oxa-pyridine Derivatives. Trop J Nat Prod Res. 2023; 7(11):5270-5278. <http://www.doi.org/10.26538/tjnpr/v7i11.36>

Official Journal of Natural Product Research Group, Faculty of Pharmacy, University of Benin, Benin City, Nigeria

3-Cyano-2-pyridones are analogous to the alkaloid ricinine, the first known alkaloid that contains a cyano group. The anticancer activity of 3-cyano-2-pyridone derivatives is exciting due to the numerous biological targets they may interact with, including phosphodiesterase 3 and the provirus integration site for the Moloney murine leukaemia virus-1 kinase and survival.^{18,19} Encouraged by recent literature observations, some new pyridine derivatives were synthesised in this study, resulting in fascinating heterocyclic frameworks that are most beneficial for the construction of various chemical libraries of compounds with a variety of functional groups for examining unique biological agents. This study was aimed at synthesising new 3-cyano-2-oxa-pyridine derivatives (4a-e) using substituted acetophenone, ethyl cyanoacetate, and aryl aldehydes in the presence of ammonium acetate. Moreover, they demonstrated anticancer efficacy against two cancer cell lines, namely cerebral glioblastoma multiforme and cervical carcinoma. The variations in biological activity induced by changes in the positions of substituted groups like H, Br, NH₂, and OCH₃ were explored as an outcome of this research. The synthesised compounds were subjected to theoretical calculations using the density-functional theory (DFT), an adverse medical device event (AMDE) assay, and by making comparisons with experimental data. These studies will provide insight into the molecular properties of novel pyridine derivatives.

Materials and Methods*Sources for cell lines and maintenance of cell cultures*

Two cancer cell lines, namely cerebral glioblastoma multiforme (AMGM5) and cervical carcinoma (HeLa), were purchased from the IRAQ Biotechnology Cell Banking Centre in Basrah and grown in RPMI-1640 treated with 10% foetal bovine serum, 100 units/mL of the antibiotic penicillin, and 100 g/mL of minocycline. The cells were

passed with Trypsin-EDTA, reseeded at 70% viability twice to three times per week, and grown at 37°C in 5% carbon dioxide (CO₂).²⁰

Synthesis of substituted 3-cyano-2-oxa-pyridines (4a-e)

A mixture of aryl-ketone (10 mmol), ethyl cyanoacetate (10 mmol), the appropriate aldehyde (1 mmol), and ammonium acetate (77 mmol) in n-butanol (20 mL) was refluxed overnight until completion (TLC eluent: hexane-ethyl acetate (6:4)), and iodine vapours were employed to see the spot. Then, the solvent was evaporated, precipitated by crushed ice, and the generated residue was washed with ethyl alcohol. The remaining residue was collected, dried, and crystallized from ethyl alcohol to yield the synthesized products.

Spectral analyses

All the chemicals were purchased from Sigma-Aldrich® and utilized without further purification. The melting points of the synthesized compounds were determined in capillary tubes utilizing the Griffin apparatus. The reaction was checked on silica gel TLC plates. Proton nuclear magnetic resonance (¹H NMR) at 400 MHz and ¹³C-NMR at 100 MHz were carried out on a Bruker® ARX-400 spectrometer at the University of Basrah, Iraq. Deuterated dimethyl sulfoxide was used as the internal solvent (¹H NMR: DMSO-d₆: δ 2.5 ppm and water at 3.35 ppm; carbon-13 (C13) nuclear magnetic resonance (¹³C NMR): DMSO-d₆: δ 39.52 ppm), and the internal standard was TMS (tetramethylsilane). At Tehran University in Iran, an Agilent® 5973 spectrometer was used to record the mass spectra of the manufactured products using the electron impact (EI) technique at a voltage of 70 eV.

Rapid cell feasibility analyses

To determine the cytotoxic effect, an MTT (3-(4, 5-dimethylthiazol-2-yl)-2, 5-diphenyltetrazolium bromide) assay was performed using 96-well plates. Trypsin was used to enzymatically separate the AMGM5 and HeLa cells, which were then gathered and standardised to a density of 1.4 at 104 cells/well to create a monolayer culture.²¹ After being seeded onto 96-well plates with 200 µl of fresh media in each well, the standardised cells were cultured for 24 hours. The cells were exposed to substances ranging from 125 to 1000 µg/mL for 24 hours at 37°C in 5% CO₂ after they had formed a single layer. The liquid above was taken out and 200 µl/well of MTT solution (0.5 mg/mL in phosphate-buffered saline [PBS]) was added after the therapy (72 hours) had ended. The monolayer culture was left unaltered in its original container. The dish was then kept at 37°C for an additional four hours. After removing the cell supernatant, 100 µl of dimethyl sulfoxide was added to each well in place of the MTT solution. The cells were cultivated for the full dissolution of the crystals at 37°C on shaking equipment. Their absorbance at 620 nm was used to measure the viability using a Biotek® PowerWave™ XS Microplate ELISA Reader (USA). Based on the dose-response curves, the IC₅₀—a measure of the concentration of a chemical that caused a 50% reduction in cell viability—was computed.^{22,23}

Predicting the in-silico absorption, distribution, metabolism, and excretion (ADME) properties

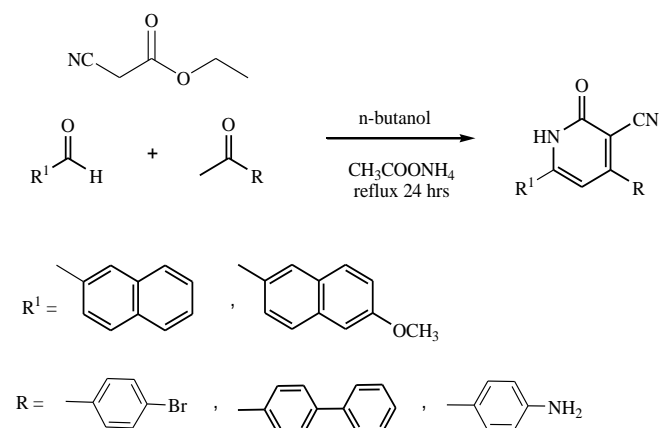
The SwissADME online^{24,25} tool was used to calculate the predicted pharmacokinetics and drug-likeness properties of the newly synthesised compounds to evaluate them as potential drug candidates.

Optimising the compounds' models and geometries

Figure 3 shows the optimised molecular geometries of the compounds calculated at the B3LYP/6-311+G(d,p) level. The computations were performed using the Gaussian 03 program,²⁶ and after the optimisation, none of the frequency computations created imaginary frequencies.

Results and discussions

3-Cyano-2-oxa-pyridine compounds are increasingly important in modern medicine, particularly in cancer therapy. To begin, to evaluate the simplicity of the one-pot multicomponent reaction^{27,28} using substituted acetophenone, ethyl cyanoacetate, and aryl aldehydes in the presence of ammonium acetate in n-butanol under reflux overnight, good yield was obtained (Scheme 1). The structures of all the resultant pyridine analogues were validated using NMR spectroscopy and mass spectrometry. 3-Cyano-2-oxa-pyridine compounds 4a-e were used to generate ¹H NMR spectra. The singlet signals at 12.93, 12.87, 12.91, and 8.36 ppm are attributed to the NH group, with the remaining protons in the correct positions. Compound 4e showed that the singlet signal at δ 3.89 ppm belongs to the NH₂ group. Furthermore, the ¹³C NMR spectra of compounds 4a-e exhibited signals at 117.0, 117.3, 117.1, 117.2, and 116.6 ppm, which were attributed to the cyano group, and signals at 160.1, 159.1, 160.5, 160.6, and 160.5 ppm attributed to the carbonyl group. The 2-D NMR analysis using HSQC was carried out for compound 4e, and it revealed a correlation among the signal at 3.92 (3H, s) ppm and the CH signal at 56.0 ppm, as well as the signal at 7.41 (1H, s) ppm and the CH signal at 106.8 ppm. The mass spectra of the 4a-e compounds revealed the presence of a molecular ion (m/z): 400.1 (M)⁺, 428.2 (M)⁺, 398.2 (M)⁺, 337.2 (M)⁺, and 367.4 (M)⁺, which corresponded to the predicted values of m/z 400.02, 428.15, 398.14, 337.12, and 367.13. Table 1 shows the physical properties and molecular formula of compounds 4a-e.



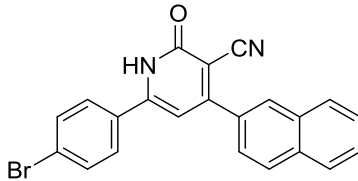
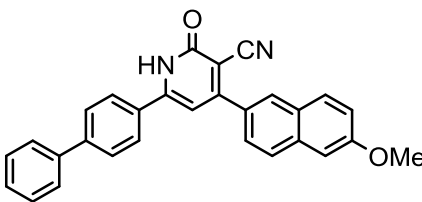
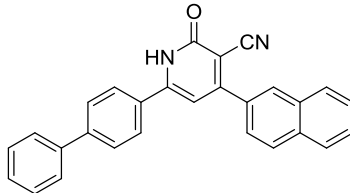
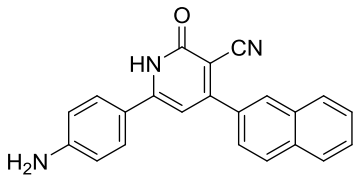
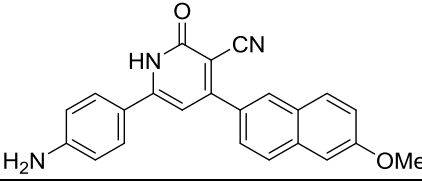
Scheme 1: Synthetic route of target pyridine compounds.

Table 1: The physical properties of prepared compounds.

Compounds	Molecular formula	M.wt g/mol	Color	Time/h	m.p (°C)	Yield (%) ^a
4a	C ₂₂ H ₁₃ BrN ₂ O	401.26	white	24	236-238 265-	88
4b	C ₂₉ H ₂₀ N ₂ O ₂	428.49	yellow	24	267 251-253	85
4c	C ₂₈ H ₁₈ N ₂ O	398.47	yellow	24	230-232 242-	80
4d	C ₂₂ H ₁₅ N ₃ O	337.38	yellow	24	244	76
4e	C ₂₃ H ₁₇ N ₃ O ₂	367.41	yellow	24		84

^aIsolated pure derivative

Table 2: Cytotoxic effects of test compounds on the AMGM5 and HeLa cell lines

Compounds	IC ₅₀ AMGM5	IC ₅₀ HeLa
4a 	656.4	558.5
4b 	---	775.6
4c 	781.5	---
4d 	----	---
4e 	374.5	615.9

*Characteristics of the synthesized compounds**6-(4-bromophenyl)-4-(naphthalene-2-yl)-2-oxo-1,2-dihydropyridine-3-carbonitrile (4a)*

It was white in colour and yielded 88% at an mp of 236-238°C, ¹H NMR (DMSO-d₆): H8 (1H, δ=7.04 ppm), H21,22 (2H, δ=7.65 ppm), H1,3 (2H, 7.76 ppm), H19 (1H, 7.84 ppm), H4,6 (2H, 7.90 ppm), H20,23 (2H, 8.05 ppm), H15 (1H, 8.11 ppm), H16 (1H, 8.34 ppm), H12 (1H, 12.93 ppm). ¹³C NMR (DMSO-d₆): C10 (δ=117.0 ppm), C8 (δ=125.4 ppm), C25 (δ=125.7 ppm), C5 (δ=125.8 ppm), C15 (δ=127.5 ppm), C16 (δ=128.2 ppm), C22 (δ=128.8 ppm), C23 (δ=128.9 ppm), C21 (δ=129.1 ppm), C20 (δ=130.3 ppm), C1,3 (δ=132.4 ppm), C19 (δ=132.9 ppm), C2 (δ=133.8 ppm), C4,6 (δ=133.9 ppm), C14 (δ=139.2 ppm), C18 (δ=142.3 ppm), C17 (δ=145.3 ppm), C7 (δ=151.7 ppm), C11 (δ=160.1 ppm), C9 (δ=162.6 ppm). MS (EI): m/z 400.1 [M]⁺, as shown in Figures 5-7.

6-([1,1'-biphenyl]-4-yl)-4-(6-methoxynaphthalen-2-yl)-2-oxo-1,2-dihydropyridine-3-carbonitrile (4b)

It was yellow in colour and yielded 85% at an mp of 265-267°C, ¹H NMR (DMSO-d₆): H33 (3H, δ=3.92 ppm), H13 (1H, δ=7.01 ppm), H23 (1H, 7.28 ppm), H21, 27 (2H, 7.44 ppm), H26, 28 (2H, 7.51 ppm), H25, 29 (2H, 7.76 ppm), H1,3,20 (3H, 7.85 ppm), H4,6,17,24 (4H, 8.01 ppm), H16 (1H, 8.29 ppm), H9 (1H, 12.87 ppm). ¹³C NMR (DMSO-d₆): C33 (δ=55.9 ppm), C11 (δ=106.3 ppm), C21 (δ=106.4 ppm), C13 (δ=117.3), C30 (δ=119.6), C23 (δ=120.1 ppm), C16 (δ=121.5 ppm), C17 (δ=125.5 ppm), C1,3 (δ=126.3 ppm), C4,6 (δ=127.3 ppm), C19 (δ=127.5 ppm), C25 (δ=127.7 ppm), C29

(δ=127.9 ppm), C27 (δ=128.3 ppm), C24 (δ=128.7 ppm), C26 (δ=129.6 ppm), C28 (δ=130.8), C20 (δ=131.2 ppm), C5 (δ=131.4 ppm), C15 (δ=134.0 ppm), C18 (δ=135.6 ppm), C7 (δ=139.2 ppm), C2 (δ=143.1 ppm), C8 (δ=144.9 ppm), C22 (151.5 ppm), C10 (δ=159.1 ppm), C12 (δ=162.8 ppm). MS (EI): m/z 428.2 [M]⁺, as shown in Figures 8-10.

6-([1,1'-biphenyl]-4-yl)-4-(naphthalen-2-yl)-2-oxo-1,2-dihydropyridine-3-carbonitrile (4c)

It was yellow in colour and yielded 80% at an mp of 251-253°C, ¹H NMR (DMSO-d₆): H8 (1H, δ=7.04 ppm), H27 (1H, δ=7.44 ppm), H22,26 (2H, δ=7.51 ppm), H28,21 (2H, δ=7.66 ppm), H25,29 (2H, δ=7.77 ppm), H19,20,23 (3H, δ=7.86 ppm), H4,6,1,3 (4H, δ=8.05 ppm), H15 (1H, δ=8.12 ppm), H16 (1H, δ=8.36 ppm), H12 (1H, δ=12.91 ppm). ¹³C NMR (DMSO-d₆): C10 (δ=117.1 ppm), C8 (δ=122.8 ppm), C30 (δ=124.9 ppm), C15 (δ=125.8 ppm), C4,6 (δ=127.3 ppm), C1,3 (δ=127.5 ppm), C16 (127.9 ppm), C22 (δ=128.2 ppm), C23 (δ=128.8 ppm), C25 (δ=128.9 ppm), C27 (δ=129.6 ppm), C29 (δ=129.8 ppm), C20 (δ=131.3 ppm), C21 (δ=132.9 ppm), C26 (δ=133.4 ppm), C28 (δ=133.9 ppm), C19 (δ=134.4 ppm), C2 (δ=136.9 ppm), C14 (δ=139.2 ppm), C18 (δ=139.4 ppm), C17 (δ=143.2 ppm), C24 (δ=144.5 ppm), C5 (δ=145.0 ppm), C7 (δ=151.4 ppm), C11 (δ=160.5 ppm), C9 (δ=162.4 ppm). MS (EI): m/z 398.2 [M]⁺, as shown in Figures 11-13.

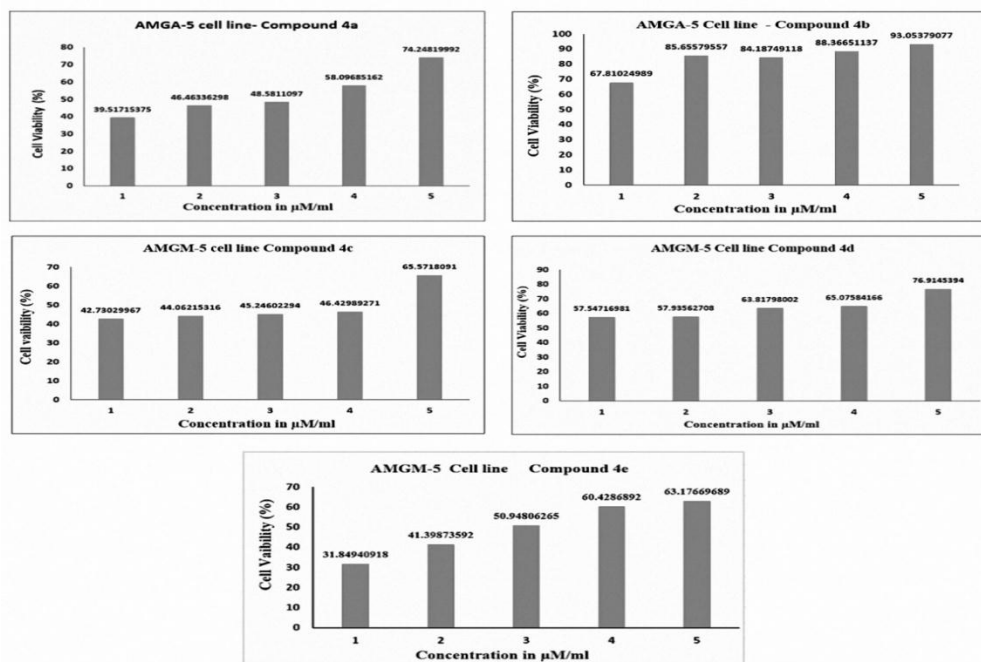


Figure 1: Cell viability assay on AMGM5 cell line for compounds 4a-e.

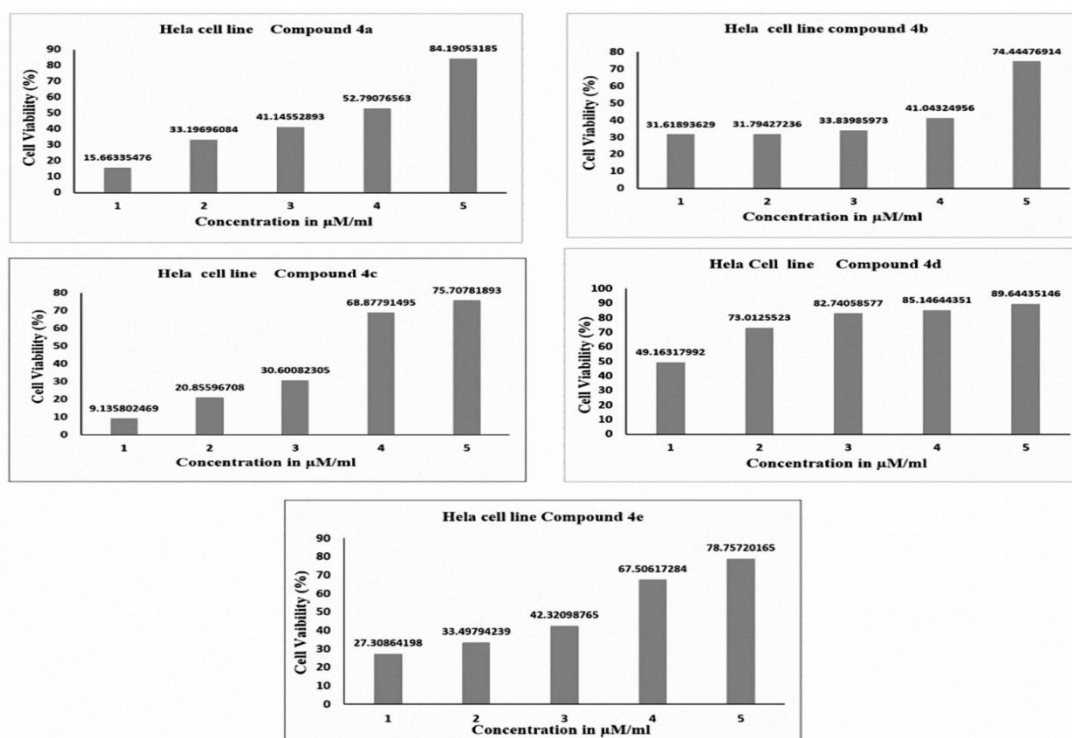


Figure 2: Cell viability assay on HeLa cell line for compounds 4a-e.

6-(4-aminophenyl)-4-(naphthalen-2-yl)-2-oxo-1,2-dihydropyridine-3 carbonitrile (4d)

It was yellow in colour and yielded 76% at an mp of 230-232°C, ¹H NMR (DMSO-d₆): H6,6' (2H, δ=2.36 ppm), H9 (1H, δ=6.47 ppm), H23,22 (2H, δ=7.48 ppm), H4,7,1,3 (4H, δ=7.59 ppm), H21 (1H, δ=7.79 ppm), H20,24 (2H, δ=7.87 ppm), H16 (1H, δ=8.00 ppm), H17 (1H, δ=8.11 ppm), H13 (1H, δ=8.36 ppm). ¹³C NMR (DMSO-d₆): C11 (δ=117.2 ppm), C9 (δ=119.7 ppm), C4,7 (121.6 ppm), C25 (δ=125.4 ppm), C2 (δ=125.6 ppm), C16 (125.9 ppm), C23 (δ=126.5 ppm), C17 (δ=127.4 ppm), C24 (δ=127.9 ppm), C22 (128.1 ppm), C21

(δ=128.3 ppm), C13 (δ=128.9 ppm), C20 (δ=129.1 ppm), C15 (δ=131.4 ppm), C19 (δ=132.3 ppm), C18 (δ=133.1 ppm), C5 (δ=147.9 ppm), C8 (δ=152.8 ppm), C12 (δ=160.6 ppm), C10 (δ=162.0 ppm). MS (ED): m/z 337.2 [M]⁺, as shown in Figures 14-16.

6-(4-aminophenyl)-4-(6-methoxynaphthalen-2-yl)-2-oxo-1,2-dihydropyridine-3 carbonitrile (4e)

It was yellow in colour and yielded 84% at an mp of 242-244°C, ¹H NMR (DMSO-d₆): H6,6' (2H, δ=3.89 ppm), H28 (3H, δ=3.94 ppm), H9 (1H, δ=4.33 ppm), H4,7 (2H, δ=7.28), H23 (1H, δ=7.45 ppm),

H21,1,3 (3H, δ =7.95 ppm), H20 (1H, δ =8.19 ppm), H17,24,16 (3H, δ =8.46 ppm). ¹³C NMR (DMSO-d₆): C28 (δ =56.0 ppm), C11 (δ =62.7 ppm), C21 (δ =100.5 ppm), C9 (δ =100.8 ppm), C4,7 (δ =106.8 ppm), C25 (δ =116.6 ppm), C23 (δ =120.5 ppm), C2 (δ =125.5 ppm), C16 (δ =125.6 ppm), C17 (δ =127.0 ppm), C24 (δ =127.1 ppm), C1,3 (δ =128.1 ppm), C19 (δ =128.2 ppm), C20 (δ =131.6 ppm), C15 (δ =135.2 ppm), C18 (δ =137.3 ppm), C5 (δ =155.4 ppm), C8 (δ =155.6 ppm), C22 (δ =160.5 ppm), C12 (δ =162.7 ppm), C10 (δ =163.2 ppm). MS (EI): m/z 367.4 [M]⁺, as shown in Figures 17-20.

In vitro anti-cancer assay

The 4a-e compounds were evaluated in vitro against two human tumour cancer cell lines, namely AMGM5 (cerebral glioblastoma multiforme) and HeLa (cervical carcinoma), using the MTT assay.²⁹ The cytotoxic potential of the compounds varied according to the cell type (Figures 1, 2). According to the results, the series of synthesised compounds demonstrated significantly enhanced cytotoxicity against AMGM5 (cerebral glioblastoma multiforme). The 4a, 4c, and 4e compounds were more susceptible to AMGM5 and had the highest potency with IC₅₀ values of 656.4, 781.5, and 374.5 μ g/mL, respectively, but the 4b and 4d compounds exhibited no activity against the growth of AMGM5 (Table 2). The 4a, 4b, and 4e compounds were the most sensitive and potent against the HeLa cell line, with IC₅₀ values of 558.5, 775.6, and 615.9 g/mL, respectively; however, the other compounds (4c and 4d) had no effect against the growth of the HeLa cell line, as shown in Table 2. Compounds with different chemical structures may have a different activity against the characteristics of tumour cells.^{30,31} According to these results, compounds with high toxicity and anti-tumour effects may have therapeutic potential.^{32,33} These findings, together with some

experimental data regarding the use of pyridine anticancer medicines,³⁴ open new avenues for drug research and development.

Predicting the compounds' absorption, distribution, metabolism, and excretion (ADME) properties

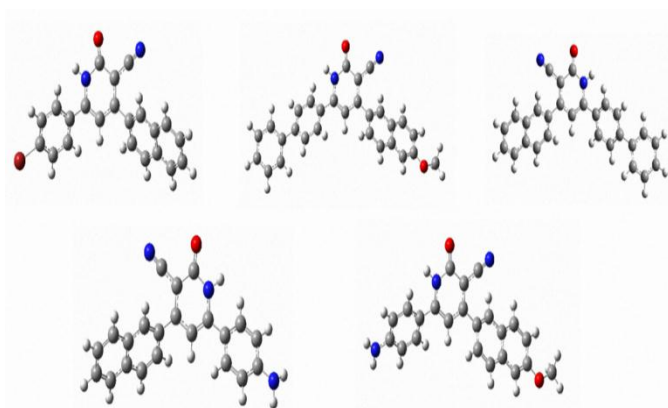
Simple approaches are desirable for predicting the ADME properties of drug candidates due to the cost and duration of in vivo investigations. Computer prediction models offer a quick and affordable technique for evaluating the potential ADMET (absorption, distribution, metabolism, excretion, and toxicity) characteristics of a drug. Table 3 shows the analytical findings for the predicted ADMET properties of the drugs. Table 3 demonstrates that every compound complied with Lipinski's criterion without exception, i.e., the topological polar surface area (TPSA) values fell below 140 (between 56.65 to 91.90). Additionally, their bioavailability score of 0.55 indicated that they were more drug-like in nature.³⁵ In contrast, the lipophilicity behaviour was demonstrated by a consensual Log Po/w in the range of 5.44 to 3.59. Although the 4c and 4d compounds had good drug-likeness, they showed less potency. Except for 4a and 4c, the 4b, 4c, and 4e compounds predictably demonstrated an ability to permeate the BBB. The 4a, 4d, and 4e compounds belonged to the class of moderately soluble compounds, while the 4b and 4c compounds fell into the category of poorly soluble compounds. On the contrary, all the compounds showed different efficacies against CYP enzymes. Unfortunately, the drug-likeness profile was not very encouraging because some of the compounds did not follow specific rules; most of the compounds showed two violations in lead-likeness due to their large molecular weights (Mwt > 350) and XLOGP3 values, which should be > 3.5. On the other hand, the compounds under study had several advantageous ADME characteristics. The pharmacokinetics and drug-like effects of the substances shifted when their chemical structures were altered.^{36,37}

Table 3: Calculated ADME properties and pharmacokinetic properties of the synthesized compounds

Parameters	Compounds				
	4a	4b	4c	4d	4e
Molecular weight (g/mol)	401.26	428.49	398.47	337.38	367.41
No. of HBAs	2	3	2	2	3
No. of HBDs	1	1	1	2	3
No. of rotatable bonds	2	4	3	2	2
TPSA(A ²)	56.65	65.88	82.67	82.67	91.90
Molar refractivity (cm ³)	107.86	132.08	125.59	104.56	
Water solubility	Moderately	Poorly	Poorly	Moderately	Moderately
Drug likeness	No; 2 violations: MW>350, XLOGP3>3.5	No; 2 violations: MW>350, XLOGP3>3.5	No; 2 violations: MW>350, XLOGP3>3.5	No; 1 violation: XLOGP3>3.5	No; 1 violation: MW>350
Consensus Log <i>P</i> _{o/w}	4.76	5.44	3.59	3.60	3.59
BBB permeant	Yes	No	Yes	No	No
CYP1A2 inhibitor	Yes	Yes	Yes	Yes	Yes
CYP2C19 inhibitor	Yes	No	Yes	Yes	No
CYP2C9 inhibitor	Yes	No	No	Yes	Yes
CYP2D6 inhibitor	No	No	No	Yes	Yes
CYP3A4 inhibitor	No	No	No	Yes	Yes
Lipinsk rule validation	Yes	Yes	Yes	Yes	Yes
Ghose	Yes	No	No	Yes	Yes
Veber	Yes	Yes	Yes	Yes	Yes
Egan	Yes	No	No	Yes	Yes
Muegge	Yes	No	No	Yes	Yes
Bioavailability Score	0.55	0.55	0.55	0.55	0.55

Table 4: Ground state properties of the compounds using B3LYP/6-311+G(d,p)

Compounds	HOMO (eV)	LUMO (eV)	ΔE (eV)	μ (eV)	χ (eV)	η (eV)	S (eV ⁻¹)	ω
4a	-6.45	-2.801	3.649	-4.6255	4.6255	1.8245	0.5480	5.8633
4b	-6.003	-2.611	3.392	-4.307	4.307	1.696	0.5896	5.4688
4c	-6.352	-2.687	3.665	-4.5195	4.5195	1.8325	0.5457	5.5732
4d	-6.101	-2.348	3.753	-4.2245	4.2245	1.8765	0.5329	4.7552
4e	-5.896	-2.312	3.584	-4.104	4.104	1.792	0.5580	4.6994

**Figure 3:** Optimized molecular geometries of compounds calculated at B3LYP/6-311+G(d,p) method.

Computational analysis

Table 4 summarizes the computed quantum chemical variables generated from the energy band gap $\Delta E = E_{\text{LUMO}} - E_{\text{HOMO}}$, such as highest occupied molecular orbital (HOMO), least unoccupied molecular orbital (LUMO), chemical potential (μ), electronegativity (χ), chemical hardness (η), chemical softness (S), and electrophilicity (ω). Figure 4 shows the atomic orbital compositions of the molecular orbitals. The calculated quantum chemical variables are shown in Table 4. The HOMO is often associated with the ability of a molecule to donate electrons. A molecule is likelier to donate electrons to suitable acceptor molecules with vacant molecular orbitals and low energy when the EHOMO value is high. The ability of a molecule to accept electrons is referred to as the ELUMO. If the ELUMO is low, the molecule is more likely to receive electrons³⁸. The 4a compound had the lowest EHOMO (-6.45 eV), according to Table 4, whereas 4e had the highest EHOMO (-5.896 eV). The 4a compound had the lowest ELUMO (-2.801 eV), whereas, 4e had the greatest ELUMO (-2.312 eV). The kinetic stability was evaluated using a simple method called the HOMO-LUMO energy difference.³⁹ High energy gap molecules are very kinetically stable and have low chemical reactivity (ΔE).⁴⁰ Because it is simpler to transfer electrons to acceptors, a molecule with a low-energy gap tends to be more reactive. A high-energy gap molecule is called a "hard molecule" since it is harder to polarize because it needs more energy to excite.⁴¹ The 4b compound was the least stable and most reactive (soft molecule). In contrast, the 4d compound was the most stable and least reactive (hard molecule), according to Table 4. The electronic μ , which accounts for the propensity of electrons to escape in an equilibrium system,⁴² was calculated using Equation (1):

$$\mu = \frac{1}{2(E_{\text{HOMO}} + E_{\text{LUMO}})} \quad (1)$$

The electrical μ of the compounds are listed in order of occurrence as $4e > 4d > 4b > 4c > 4a$. The property known as χ , which indicates the capacity of an atom or group of atoms to attract electrons, was calculated using Equation (2):

$$\chi = -\frac{1}{2(E_{\text{HOMO}} + E_{\text{LUMO}})} \quad (2)$$

The χ scale running from modest to large was $4e < 4d < 4b < 4c < 4a$.⁴³ The chemical hardness (η) or resistance of a molecule to changes in electron distribution determines the stability and reactivity of a chemical system.⁴² The formula for hardness is given in Equation (3):

$$\eta = \frac{1}{2(E_{\text{HOMO}} - E_{\text{LUMO}})} \quad (3)$$

According to the data, unlike the 4b compound, which was more unstable (softer) and reactive, the 4d compound was more stable (harder) and less reactive. Softness, which is the opposite of hardness, can be calculated using Equation (4)⁴⁴:

$$S = \frac{1}{\eta} \quad (4)$$

A softer species (atom/molecule) has a propensity to be more polarizable and magnetic.⁴⁵ According to Table 4, the 4b compound exhibited greater softness and polarizability, while the 4d compound had less softness and polarizability. The global ω index is a metric that can determine the ability of a molecule to pick up electrons,⁴⁶ and can be calculated using Equation (5):

$$\omega = \frac{\mu^2}{2\eta} \quad (5)$$

The ω scale classifies organic molecules as "strong electrophiles". For weak electrophiles, $\omega < 0.8$ eV; for moderate electrophiles, $0.8 < \omega < 1.5$ eV; for strong electrophiles, $\omega > 1.5$ eV; and for super electrophiles, $\omega > 4.0$ eV.^{47, 48} The final species exhibited a very high level of polar reaction reactivity.^{49, 50} The ω characteristic in descending order was as follows: $4a > 4c > 4b > 4d > 4e$.

Conclusion

A series of 3-cyano-2-oxa-pyridine derivatives was effectively synthesized via a one-pot multicomponent synthesis. The most active compounds in the derivative series against AMG5 and HeLa cell lines were the 4a and 4e compounds. HeLa and AMG5 cell lines' growth suppression was not inhibited by compound 4d. The 4d molecule was discovered to be the most stable and least reactive, based on the molecular orbital and electronic structures displayed. The 4b compound, on the other hand, was discovered to be the most reactive and least stable. The established drug-likeness guidelines were developed and the ADMET was predicted using the SwissADME program.

Conflict of Interest

The authors declare no conflict of interest.

Authors' Declaration

The authors hereby declare that the work presented in this article is original and that any liability for claims relating to the content of this article will be borne by them.

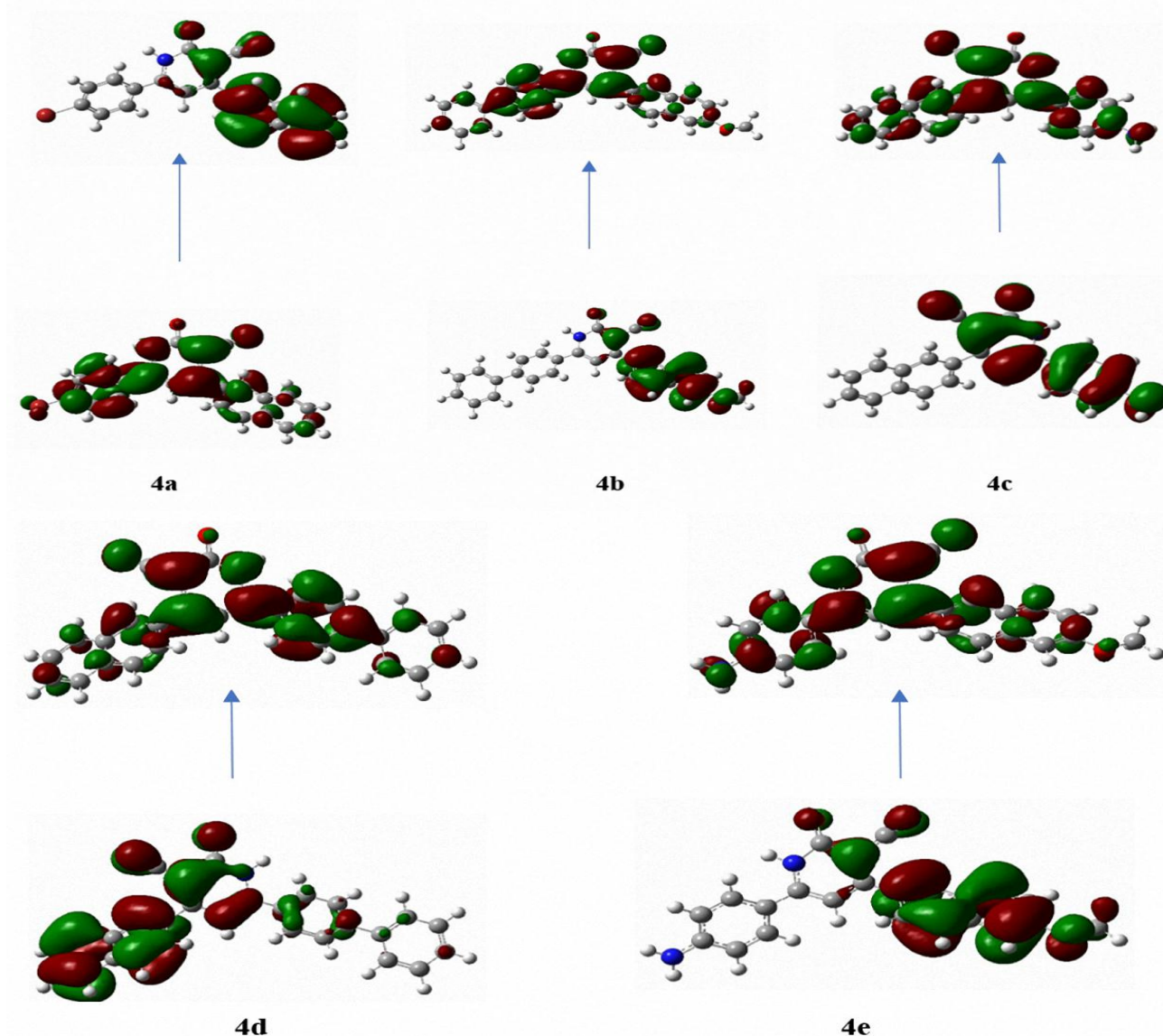


Figure 4: HOMO–LUMO orbital diagram of compounds

Acknowledgements

The authors would also like to thank Dr Ali Abdul Lateef from the Faculty of Biology, College of Education for Pure Sciences, University of Basrah, Iraq for his support in determining the toxicity of compounds.

References

- Hovhannisyan AA, Aristakesyan LH, Hakobyan RM, Melikyan GS. Synthesis of new 3-cyanopyridine-2(1H)-ones with unsaturated substituents AT C-4. *Proc. of the Yerevan State Univ. Chem. Biol.* 2015; 2: 9–13.
- Pareshkumar UP, Vipul PG, Purohit DM, Patolia VN. Synthesis and biological evaluation of some new cyano pyridine derivatives. *J. Chem. Pharm. Res.* 2015; 7(1):182-186.
- Ahmed M, Mona M, Hassan A, Ola R, Omima S, Mohamed S, Zaki AS, Hayam A. New 3-Cyano-2-Substituted Pyridines Induce Apoptosis in MCF 7 Breast Cancer Cells. *Mol.* 2016; 21: 230.
- Azzarito V, Long K, Murphy NS, Wilson AJ. Inhibition of α -helix-mediated protein–protein interactions using designed molecules. *Nat Chem.* 2013; 5(3): 161-173.
- Marzouk AA, Bass AK, Ahmed MS, Abdelhamid AA, Elshaiyer YA, Salman AM. Design, synthesis and anticonvulsant activity of new imidazolidindione and imidazole derivatives. *Bioorg. Chem.* 2020; 101: 104020.
- Murata T, Shimizu K, Narita M, Manganiello VC, Tagawa T. Characterization of phosphodiesterase 3 in human malignant melanoma cell line. *Anticancer Res.* 2002; 22(6A): 3171-3174.
- Teague SJ. Synthesis of heavily substituted 2-aminopyridines by displacement of a 6-methylsulfinyl group. *J. Org. Chem.* 2008; 73(24): 9765-9766.
- Bass AKA, El-Zoghbi MS, Abdelhafez EMN, Mohamed MF, Badr M, Abuo-Rahma GE-DA. Comprehensive review for anticancer hybridized multitargeting HDAC inhibitors. *Eur. J. Med. Chem.* 2021; 209: 112904.
- Bringmann G, Reichert Y, Kane VV. The total synthesis of streptonigrin and related antitumor antibiotic natural products. *Tetrahedron* 2004; 16(60): 3539-3574.

10. Zhou Y, Kijima T, Kuwahara S, Watanabe M, Izumi T. Synthesis of ethyl 5-cyano-6-hydroxy-2-methyl-4-(1-naphthyl)-nicotinate. *Tetrahedron Lett.* 2008; 49(23): 3757-3761.
11. Faidallah HM, Rostom SA, Badr MH, Ismail AE, Almohammadi AM. Synthesis of Some 1, 4, 6-Trisubstituted-2-oxo-1, 2-dihydropyridine-3-carbonitriles and Their Biological Evaluation as Cytotoxic and Antimicrobial Agents. *Arch. Pharm. Chem. Life Sci.* 2015; 348: 824-834.
12. Al-Etaibi AM, El-Asasery MA. A comprehensive review on the synthesis and versatile applications of biologically active pyridone-based disperse dyes. *Int. J. Environ. Res. Public Health.* 2020; 17(13): 4714.
13. Mamedov I, Naghiyev F, Maharramov A, Uwangue O, Farewell A, Sunnerhagen P, *et al.* Antibacterial activity of 2-amino-3-cyanopyridine derivatives. *Mendeleev Commun.* 2020; 30: 498-499.
14. Hanaa MH, Mohamed MA. Anti-inflammatory and analgesic activities of some newly synthesized pyridinedicarbonitrile and benzopyranopyridine derivatives. *Acta Pharm.* 2008; 58(2): 175-186.
15. Al-Omar MA, Amr AE, Al-Salahi RA. Anti-inflammatory, analgesic, anticonvulsant and antiparkinsonian activities of some pyridine derivatives using 2,6-disubstituted isonicotinic acid hydrazides. *Arch. Pharm. Chem. Life Sci.* 2010; 343: 648-656.
16. Amr AE, Sayed HH, Abdulla MM. Synthesis and reactions of some new substituted pyridine and pyrimidine derivatives as analgesic, anticonvulsant and antiparkinsonian agents. *Arch. Pharm. Chem. Life Sci.* 2005; 338: 433-440.
17. Ismail MM, Farrag AM, Harras MF, Ibrahim MH, Mehany AB. Apoptosis: A target for anticancer therapy with novel cyanopyridines. *Bioorg. Chem.* 2020; 94: 103481.
18. Eman M. Fiefel, Hebat-Allah S. Abbas, Randa E. Abdel Mageid and Wafaa A. Zachary, Synthesis and Cytotoxic Effect of Some Novel 1,2-Dihydropyridin-3-carbonitrile and Nicotinonitrile Derivatives. *Mol.* 2016; 21(1): 30.
19. Ahmed HS, Eman RK, Manal MA, Mohamed S. A Review on The Chemistry of Nicotinonitriles and Their applications. *Egypt. J. Chem.* 2021; 64: 4509 – 4529.
20. Ali AAA, Khalid ASA, Ahmed MA. Cytotoxic effects of CeO₂ NPs and β- carotene and their ability to induce apoptosis in human breast normal and cancer cell lines. *Iraqi J. Sci.* 2022; 63: 3.923-937.
21. Falih SM, Al-Saray ST, Alfari AA, Al-Ali A.A. The synergistic effect of eucalyptus oil and retinoic acid on human esophagus cancer cell line SK-GT-4. *Egypt. J. Med. Hum. Genet.* 2022; 23:70.
22. Al-Shammari AM, Al-Esmael WN, Al-Ali AA, Hassan AA, Ahmed AA. Enhancement of Oncolytic Activity of Newcastle Disease Virus Through Combination with Retinoic Acid Against Digestive System Malignancies. *Mol. Ther.* 2019; 27(4S1):126-127.
23. Freshney RI. *Culture of Animal Cells: A Manual of Basic Technique and Specialized Applications.* 6th ed. Wiley-Blackwell. 2010; P732.
24. Saima M, Rahat A, Sumreen H, Muhammad UI, Asma A, Nimrah Z, Shabana N, Mubashera S. Integrating In Silico and In Vitro Approaches to Screen the Antidiabetic Properties from *Tabernaemontana divaricata* (Jasmine) Flowers. *Evid. Based Complement. Alternat. Med.* 2022; 9: 1-17.
25. Anees P, Khurshed A. Synthesis and biological evaluation of coumarin-quinone hybrids as multifunctional bioactive agents. *Admet Dmpk.* 2023; 11(1): 81-96.
26. Frisch MJ, Trucks GW, Schlegel HB, Scuseria GE, Robb MA, Cheeseman JR, Scalmani G, Barone V, Petersson GA, Nakatsuji H, Li X, Caricato M, Marenich AV, Bloino J, Janesko BG, Gomperts R, Mennucci B, Hratchian HP, Ortiz JV, Izmaylov AF, Sonnenberg JL, Williams-Young D, Ding F, Lipparini F, Egidi F, Goings J, Peng B, Petrone A, Henderson T, Ranasinghe D, Zakrzewski VG, Gao J, Rega N, Zheng G, Liang W, Hada M, Ehara M, Toyota K, Fukuda R, Hasegawa J, Ishida M, Nakajima T, Honda Y, Kitao O, Nakai H, Vreven T, Throssell K, Montgomery JA, Peralta JE, Ogliaro F, Bearpark MJ, Heyd JJ, Brothers EN, Kudin KN, Staroverov VN, Keith TA, Kobayashi R, Normand J, Raghavachari K, Rendell AP, Burant JC, Iyengar SS, Tomasi J, Cossi M, Millam JM, Klene M, Adamo C, Cammi R, Ochterski JW, Martin RL, Morokuma K, Farkas O, Foresman JB, Fox DJ. Gaussian 16, Revision C.01, Gaussian, Inc., Wallingford CT, 2016.
27. Akbar M, Sajad A, Mohammad AB. Convenient, multicomponent, one-pot synthesis of highly substituted pyridines under solvent-free conditions. *Synth. Commun.* 2016; 1-16.
28. Sobhi MG, Zeinab AM, Mohamad RA, Hassan MA, Hatem MG, Mahmoud ME. One-Pot Synthesis of New Thiadiazolyl-Pyridines as Anticancer and Antioxidant Agents. *J. Heterocyclic Chem.* 2018; 55(2): 530-536.
29. Amr KAB, Elshimaa MNA, Mona SE, Mamdouh FAM, Mohamed B, Gamal El-Din AAR. 3-Cyano-2-oxa-pyridines: a promising template for diverse pharmacological activities. *J. Adv. Biomed. Pharm. Sci.* 2021; 4: 81-86.
30. Mohammed A, Hassan AA. Novel pyridine and pyrimidine derivatives as promising anticancer agents: A review. *Arab. J. Chem.* 2022; 15(6): 103846.
31. Sourav De, Ashok KSK, Suraj KS, Sabnaz K, Nandan S, Subhasis B, Sanjay D. Pyridine: the scaffolds with significant clinical diversity. *RSC. Adv.* 2022; 12: 15385-15406.
32. Alaa MA, Abrar AB. Synthesis and antiproliferative activity studies of new functionalized pyridine linked thiazole derivatives. *Arab. J. Chem.* 2021; 14: 102914.
33. Sahu R, Mishra R, Kumar R, Chandana MS, Mazumder A, Kumar A. Pyridine Moiety: Recent Advances in Cancer Treatment. *Indian J. Pharm. Sci.* 2021; 83(2): 162-185.
34. Yong L, Zhi-YH, Dong L, Chun-LZ, Yan-FL, Yan W. The Expanding Role of Pyridine and Dihydropyridine Scaffolds in Drug Design. *Drug Des. Devel. Ther.* 2021; 15: 4289.
35. Lynda G, Rachid C, Mohammed L, Paul M. Synthesis, characterization of some substituted Quinolines derivatives: DFT, computational, in silico ADME, molecular docking and biological activities. *Chem. Data Collect.* 2023; 43:100977.
36. Ayesha N, Faisal A O, Asia N A, Aqeel I, Abdul H, Syed A A S, Jamshed I, Zainul A Z. Exploring Novel Pyridine Carboxamide Derivatives as Urease Inhibitors: Synthesis, Molecular Docking, Kinetic Studies and ADME Profile. *Pharm.* 2022; 15: 1288.
37. Mohamed R, Asmaa O, Halima H, Burak T, Abdelhadi H, El Hassane A, Elyor B, Mohammed A A, Abdelkader Z, Brahim L. Synthesis, bioinformatics and biological evaluation of novel pyridine based on 8-hydroxyquinoline derivatives as antibacterial agents: DFT, molecular docking and ADME/T studies. *J. Mol. Struct.* 2021; 1244: 130934.
38. Yong L, Zhi-YH, Dong L, Chun-LZ, Yan-FL, Yan W. The Expanding Role of Pyridine and Dihydropyridine Scaffolds in Drug Design. *Drug Des. Devel. Ther.* 2021; 15: 4289.
39. Gökhan G, Semra B. Quantum chemical study of some cyclic nitrogen compounds as corrosion inhibitors of steel in NaCl media. *Corros. Sci.* 2009; 51(8): 1876-1878.
40. Jun-ichi A. Correlation found between the HOMO-LUMO energy separation and the chemical reactivity at the most reactive site for isolated-pentagon isomers of fullerenes. *Phys. Chem. Chem. Phys.* 2000; 2(14):3121-3125.
41. Marzieh M, Abolfazl S, Khalil P, Ahmad RO, Farhad H. Theoretical investigations on the HOMO-LUMO gap and global reactivity descriptor studies, natural bond orbital, and nucleus-independent chemical shifts analyses of 3-

- phenylbenzo[d] thiazole-2(3H)-imine and its para-substituted derivatives: Solvent and substituent effects. *J. Chem. Res.* 2021; 147–158.
42. David P, Jyotirmoy D, Christian VA, Utpal S. Theoretical Investigation of Electronic, Vibrational and Nonlinear Optical Properties of 4-fluoro-4- hydroxybenzophenone. *Spectrosc. Lett.* 2017; 50: 4.
 43. Selma ŠH, Mirsada S, Huriya DČ, Snezana T, Suncica R, Dzenita S, Davorka Z. DFT study and microbiology of some coumarin-based compounds containing a chalcone moiety. *J. Serb. Chem. Soc.* 2014;79 (4): 435–443.
 44. Cihat H, Müşerref Ö, Mehmet EM. Detonation Parameters of the Pentaerythritol Tetranitrate and Some Structures Descriptors in Different Solvents - Computational Study. *Düzce University J. Sci. Technol.* 2021; 9: 1227-1241.
 45. Richard M, Lo P, Terrence G. Molecular Mechanisms of Aldehyde Toxicity: A Chemical Perspective. *Chem. Res. Toxicol.* 2014; 27(7): 1081–1091.
 46. Chattaraj PK, Arun Murthy TV, Giri S, Roy DR. A connection between softness and magnetizability. *J. Mol. Struct.* 2007; 813: 63-65.
 47. Andrew RJ, Timothy CJ, Douglas WS. The global electrophilicity index as a metric for Lewis acidity. *Dalton Trans.* 2018; 47: 7029-7035.
 48. Al Shuhaib Z, Hussein K A, Ismael S M. Synthesis of New Pyrimidine Derivatives, Study of Anti-Cancer Activity, Structural Properties, and Molecular Docking. *Russian J. Gen. Chem.* 2023; 93(5): 1171–1180.
 49. Mar R-G, Alejandro S S, Luis R D. Electrophilicity and nucleophilicity scales at different DFT computational levels. *J. Phys. Org. Chem.* 2023; 36: e4503.
 50. Luis RD, Mar RG, Patricia P. Applications of the Conceptual Density Functional Theory Indices to Organic Chemistry Reactivity. *Mol.* 2016; 21(6): 748.